

## Monte Carlo simulations of the distribution of Ar and other noble-gas atoms in high-pressure solid N<sub>2</sub>

E. P. van Klaveren,\* J. P. J. Michels, and J. A. Schouten

*Van der Waals-Zeeman Institute, University of Amsterdam, Valckenierstraat 65, 1018 XE Amsterdam, The Netherlands*

(Received 8 October 1999)

The distribution of argon and other noble-gas atoms over the two types of lattice sites in the nitrogen crystal at high pressure, and its consequences for the phase behavior, has been investigated with Monte Carlo simulations as a function of  $p$ ,  $T$ , and  $x_{\text{Ar}}$ . We have used  $(N,p,T)$  simulations, with an additional unphysical move, consisting of a simultaneous identity change of two unlike molecules (a “swap” move). To speed up the calculation, orientational biased sampling was performed. The preference of the guest atoms for the  $a$  sites turns out to be stronger in the  $\delta^*$  phase than in the  $\varepsilon^*$  phase. Within the  $\delta^*$  phase, three temperature regions exist. At low temperatures, the preference for the  $a$  sites is nearly complete and independent of  $T$ . At somewhat higher temperatures, the preference for the  $a$  sites rapidly decreases as a function of  $T$ . Above this region, only a small decrease towards a random distribution is observed. For 5% argon, this general behavior is independent of pressure. A larger pressure results in a stronger preference for the  $a$  sites. In contrast, increasing the Ar content within the same phase results in a less profound preference. For smaller noble-gas atoms this preference is stronger. The results are in qualitative agreement with experiments.

### I. INTRODUCTION

Mixed molecular crystals of simple components, such as  $(\text{N}_2)_{1-x}\text{-Ar}_x$ , constitute a model system for studying the influence of isotropic impurities on the orientationally ordered and disordered phases of a system of anisotropic molecules. Since the sizes of the two species, one spherical and one nearly spherical, are about equal, one may expect that the Ar atoms dissolve substitutionally in the N<sub>2</sub> lattice.

In the pressure range around 10 GPa, the solid phases of pure N<sub>2</sub> show interesting behavior.<sup>1</sup> At low temperatures the  $\varepsilon$  phase has a trigonal (rhombohedral) lattice structure with orientationally ordered molecules (space group  $R\bar{3}c$ ). This phase is regarded as a trigonal distortion of the high-temperature  $\delta$  phase, which has a cubic crystal lattice (space group  $Pm\bar{3}n$ ). The  $\delta$  phase reveals two types of orientational disorder. Of the eight lattice sites in the unit cell, the molecules in the center and on the corners of the cell ( $a$  sites, site symmetry  $m\bar{3}$ ) exhibit isotropic orientational disorder (“spheres”), while the six molecules in the faces of the cell ( $c$  sites, site symmetry  $\bar{4}m2$ ) exhibit planar orientational disorder (“disks”). Schematic pictures of the two phases are given in Fig. 2 of Ref. 3.

A marked discontinuity in the slope of the vibrational frequency shift as a function of temperature along a quasi-isobar has been detected, which has been interpreted as a second-order transition.<sup>2</sup> Monte Carlo (MC) calculations<sup>3</sup> made clear that as a result of a cascade process in the orientational delocalization of the *disks*, the vibron frequencies of the *sphere* molecules change in the way observed experimentally. At lower temperatures, the orientations of the disk molecules are localized within the plane (see, e.g., Fig. 7 of Ref. 3), and at higher temperatures they are delocalized within the plane. Thus, the Raman measurements reveal the transition from a localized  $\delta^*$  phase ( $\delta_{\text{loc}}^*$ , an asterisk denotes the mixed phase) to a  $\delta^*$  phase with increased rotational freedom ( $\delta_{\text{rot}}^*$ ). Recently, there is evidence that this transition is a weak first-order transition.<sup>4</sup>

Experimental high-pressure studies of the N<sub>2</sub>-Ar mixture<sup>5,6</sup> showed that the Ar atoms dissolve substitutionally in the lattice; moreover, these atoms are preferably located at the  $a$  sites. At low temperatures, this preference is very strong and appears to be temperature independent. At a threshold temperature, the preference for the spheres decreases rapidly with increasing temperature.<sup>6</sup> However, even at high temperatures, the preference for the  $a$  sites is obvious. Moreover, at higher pressures it is stronger. Nevertheless, for the 25% Ar mixture, a superstructure with a complete occupation of the  $a$  sites by Ar atoms as reported in Ref. 5 was not found in Ref. 6. The  $p$  and  $T$  dependence is rather surprising, since the pressures are high, and the activation energies necessary for a molecule to diffuse are much larger at higher pressures. On the other hand, a redistribution can be readily obtained after displacements of only a molecular distance, since the  $c$  sites are the nearest-neighbor sites of the  $a$  sites. Therefore, small diffusion constants may result in a significant redistribution over the two types of lattice sites within a short time. Moreover, crystal defects may contribute indirectly to the effect.

Previous simulations<sup>7</sup> showed that in the  $\delta^*$  phase, the calculated volume as well as the energy are smaller for a distribution of the Ar atoms over the  $a$  sites than over the  $c$  sites, or a random distribution. These differences are smaller in the  $\varepsilon^*$  phase.

In simulations at 7 GPa with  $T > 50$  K with all Ar atoms randomly distributed over the  $a$  lattice sites,<sup>8</sup> the N<sub>2</sub> molecules at the sphere sites exhibit more or less orientational freedom for all temperatures and Ar mole fractions  $x$ . For  $x < 0.12$ , the orientational behavior is similar to that in pure N<sub>2</sub>. For larger  $x$ , a new phase was found, in which the disks exhibit orientational order (an orientationally ordered  $\delta^*$ -like phase,  $\delta_{\text{oo}}^*$ ). At constant  $p$  the transition from this ordered phase to the more disordered  $\delta^*$  phases occurs at higher temperatures with increasing  $x$ ; the phase is more stable with increasing Ar content.

The influence of the Ar molecules on the transitions be-

tween the various  $\delta^*$  phases and on the  $\varepsilon^*$ - $\delta^*$  transition was found to be threefold. First, the  $\varepsilon^*$ - $\delta_{\text{loc}}^*$  transition shifts rapidly to lower temperatures with  $x$ : it has vanished for  $x \geq 0.05$ . Second, for  $x \geq 0.12$ , the  $\delta_{\text{oo}}^*$  phase appears. The transition from this phase to the other  $\delta^*$  phases shifts to higher temperatures with increasing  $x$ . Third, the temperature of the onset as well as the completion of the orientational cascade process, responsible for the  $\delta_{\text{loc}}^*$ - $\delta_{\text{rot}}^*$  transition, is independent of composition.

Although in previous simulations the molecules were allowed to move freely through the system, in high-density systems such as (high-pressure) solids, the free-energy barriers for a molecule to move through the system are too high. Thus, in straightforward simulations one cannot probe the preference for any of the crystallographic sites of the molecular species of the mixture. The distribution over the lattice sites remains the same during the simulation, i.e., the same as in the starting configuration.

In order to investigate the redistribution of Ar atoms as observed in experiments, we have performed simulations in which a redistribution may occur by so-called ‘‘unphysical’’ moves. We have studied such a redistribution as a function of  $p$ ,  $T$ , and  $x$ . Moreover, we have investigated whether such a redistribution is correlated with the orientational delocalization. As in the previous work, these results were obtained on the  $\text{N}_2$ -rich side ( $0 \leq x \leq 0.25$ ) for temperatures above 50 K, in the pressure region where the  $\varepsilon$  and  $\delta$  phases exist in pure  $\text{N}_2$ .

## II. METHOD AND POTENTIAL MODEL

The distribution of the noble-gas (argon) atoms will be quantified by  $y_a$ , the fraction of atoms at the  $a$  sites. Note that this parameter equals 0, 1, and 0.25, corresponding to a complete preference for the  $c$  sites, the  $a$  sites, and no preference, respectively. One way of determining the preferred distribution in a MC simulation is to perform unphysical moves, in which a simultaneous identity change of two unlike molecules is attempted (a ‘‘swap’’). Of course, the usual trial moves in position, orientation, and box parameters are also performed. For the  $\text{N}_2$ -Ar system, such a swap move consists of the following steps:

- (1) Select at random one Ar atom and one  $\text{N}_2$  molecule.
- (2) Interchange the particles, while giving the  $\text{N}_2$  molecule a new, random orientation.
- (3) Calculate the Boltzmann factor of the energy difference and accept/reject as in usual Metropolis sampling.

In this way, the mixed crystal can relax to an equilibrium configuration, i.e., a configuration with a distribution of Ar atoms over the  $a$  and  $c$  sites of the  $\text{N}_2$   $Pm\bar{3}n$  lattice that corresponds to a free-energy minimum. This method is somewhat similar to the semigrand ensemble, in which, at a certain point in the simulation, an attempt is made to change a single particle’s identity.<sup>9,10</sup> In our case, for a simultaneous identity change of two particles, there are no calculations with the chemical potential involved. Note that with this method the physical mechanisms for a redistribution cannot be investigated; one can only determine the thermodynamically favored distribution and its dependence on the thermodynamic state.

In practice, the acceptance ratios for the swapping of the

molecules were very low, in most cases less than 0.1%. Therefore, extremely long runs should be performed before the system has relaxed to equilibrium. Instead of using the straightforward scheme, a technique called orientational bias<sup>10,11</sup> is exploited to enhance the acceptance, without much additional computing time. In this orientational bias scheme, instead of one random orientation several random orientations are given to the  $\text{N}_2$  molecule at the new position. The orientation corresponding with the largest Boltzmann factor is given the largest probability to be selected. Apart from the orientation-independent Ar contribution, steps for the above scheme become the following:

- (1) Select one Ar atom and one  $\text{N}_2$  molecule, both at random.
- (2) Interchange the particles, while giving the  $\text{N}_2$  molecule  $N$  random orientations.
- (3) At the new location, calculate the Boltzmann factor of these orientations, and the Rosenbluth factor  $W = \sum_{i=1}^N e^{-\beta B_i}$  (i.e., the sum over the orientations).
- (4) At the old location, calculate the Boltzmann factor of the original orientation and of  $N-1$  random orientations, as well as the Rosenbluth factor (where the sum over orientations includes the original orientation).
- (5) Accept/reject with  $W_{\text{new}}/W_{\text{old}}$ , as is usually done with the Boltzmann factor.
- (6) At the new location, an  $\text{N}_2$  orientation is selected with its Boltzmann weight.

For the Ar contribution, the traditional scheme is used, thus  $W = e^{-\beta E_{\text{Ar}}} \sum e^{-\beta E_{i,\text{N}_2}}$ , the asterisk indicating that the Ar- $\text{N}_2$  interaction for the two molecules in question is excluded. It does not take too much effort to demonstrate that this scheme satisfies the Boltzmann distribution.<sup>10</sup> The orientational bias scheme enhances the acceptance to typically 1% to 20%, depending strongly on  $p$  and  $T$ .

The acceptance ratio also depends on the momentary distribution over the lattice sites, and the degree of preference. For example, if in  $\delta^*$ - $\text{N}_2$  the Ar atoms have a very strong preference for the  $a$  sites, while starting a calculation with all Ar atoms at the  $c$  sites, then for the first few steps the acceptance ratio is very large, since the Ar atoms are driven to the  $a$  sites. However, once equilibrium is reached, the acceptance drops significantly. Despite such a small acceptance ratio, approximate conclusions about the preferential locations of the atoms can even be drawn by starting with different Ar distributions. For instance, if one starts with a distribution over the  $c$  sites, and during a simulation most Ar atoms have migrated to the  $a$  sites, then, even with a low acceptance ratio and without reaching equilibrium, one can conclude that the Ar atoms prefer the  $a$  sites.

We have used initial configurations with three distributions: a random distribution over the  $a$  sites, over the  $c$  sites, and over both the  $a$  and the  $c$  sites. Obviously, the initial distribution of the Ar atoms should not affect the final results for a properly equilibrated simulation.

The simulations have been performed in the  $(N,p,T)$  ensemble with periodic boundary conditions, i.e., in addition to the trial translations, rotations and swap moves, a deformation of the simulation cell is attempted.<sup>12,13</sup> Occasionally, the correlations of the calculated quantities were checked,<sup>14,15</sup>

the error in  $y_a$  is estimated to be less than 0.05 for all cases. The simulations involved  $10^4$ – $10^6$  MC cycles. The total number of molecules was  $N = N_{\text{Ar}} + N_{\text{N}_2} = 512$ . Except where indicated, we have used the  $\varepsilon^*$ -N<sub>2</sub> structure for the primary configuration, since this structure has the possibility to transform spontaneously to the  $\delta$  structure in pure N<sub>2</sub> with  $(N, p, T)$  simulations. The N<sub>2</sub>-N<sub>2</sub> interaction was modeled by the Eters potential,<sup>16</sup> and a correction for the anisotropy of the site-site interaction was included.<sup>3</sup> The Ar-Ar and Ar-(N-site) interactions were modeled by an exp-6 potential.<sup>8</sup> These potentials include dispersion forces, short-range repulsion, and a quadrupolar Coulomb interaction for the N<sub>2</sub> molecules; details have been published elsewhere.<sup>8</sup> Also the definitions of the molecular angles and the method for calculating vibron frequencies have been presented in Ref. 8. To our knowledge, the potential model, used for N<sub>2</sub>, gives the best agreement with thermodynamic and structural data.

Note that for the  $\varepsilon^*$  phase, the crystallographic lattice sites are the  $2a$  (site symmetry 32) and  $6e$  (site symmetry 2) lattice sites, where the  $e$  sites correspond with the  $c$  sites in the  $\delta^*$  phase. Therefore, technically one should speak of the  $a$  and  $e$  sites in the  $\varepsilon^*$  phase. Since our simulation cell can transform from the  $\varepsilon^*$  to the  $\delta^*$  structure during a single run, we will always refer to these sites as the  $a$  and  $c$  sites when discussing the atomic distributions, to avoid elaborate and self-evident digressions.

In the next section, it will turn out that the Ar atoms show a preference for the  $a$  sites. Apart from this preference, there might be an additional preferential distribution of the Ar atoms over specific  $a$  sites. A study of several configurations (snapshots) in equilibrium does not reveal any preferential distribution over specific  $a$  sites for the compositions investigated. Moreover, a simulation that starts with a random distribution over the  $a$  sites gives a low swap acceptance, independent of the initial distribution. The cause of the sudden decrease of the acceptance ratio as (nearly) all Ar atoms have migrated should be found in the decrease of the volume: in general, the volume decreases as an Ar atom has migrated from a  $c$  site to an  $a$  site. If, with the Ar distribution already close to equilibrium two molecules are interchanged, there is a considerable probability for a large increase in energy. In such cases, one cannot be sure that the equilibrium distribution is obtained, unless infinitely long runs are performed. Whether equilibrium has been reached can be checked by starting a simulation with the Ar atoms distributed over the  $a$  sites, and one with the Ar atoms distributed over the  $c$  sites. For the data at the lowest temperatures we have checked whether the Ar distribution is in equilibrium. If this was the case, we assumed that for higher  $T$  this was also the case. Additional checks confirmed this.

### III. RESULTS

#### A. General

Figure 1 shows  $y_a$  as a function of the number of MC steps for three compositions at 4 GPa and 100 K. The figure shows that for all three compositions the final distribution is independent of the initial distribution. The equilibration time and the fluctuations in  $y_a$  increase with decreasing  $x$ ; this is probably due to the smaller statistics obtained for smaller  $x$ .

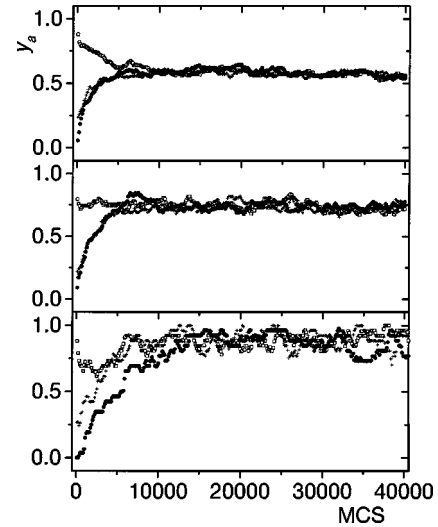


FIG. 1. The occupation level of the  $a$  sites as a function of the number of MC steps for (from top to bottom)  $x=0.25$ ,  $x=0.15$ , and  $x=0.05$  at  $(T=100$  K and  $p=4$  GPa) for three different starting distributions: random over the  $a$  sites ( $\square$ ), random over the  $c$  sites ( $\bullet$ ), and random over both the  $a$  and  $c$  sites ( $+$ ). In these runs, the  $\varepsilon^*$  phase transformed to the  $\delta^*$  phase.

An investigation of the structure (box lengths and box angles, rms displacement values, orientational distribution functions) shows that during these runs the  $\varepsilon^*$  phase spontaneously transforms to the  $\delta^*$  phase for all three compositions. The equilibrium result for  $x=0.05$  is shown in Fig. 2.

When starting with the  $\varepsilon^*$  phase, at low temperatures this phase remains stable (the open symbols in Fig. 2). Within the  $\varepsilon^*$  phase, the Ar atoms preferentially occupy the  $a$  sites, although the preference is not very pronounced. At somewhat higher temperatures, the  $\varepsilon^*$  phase transforms to the  $\delta_{\text{loc}}^*$  phase (closed symbols in Fig. 2 denote the  $\delta^*$  phase). As demonstrated in Fig. 2, the  $\varepsilon^*$ - $\delta^*$  transition corresponds with a large increase of preference for the  $a$  sites. In the simulation, the transition occurs at 85, 125, and 155 K for 4, 7, and 10 GPa, respectively. These transitions are all below the simulated  $\varepsilon$ - $\delta$  transition temperatures for pure N<sub>2</sub> (about 90, 140, and 190 K, respectively). Upon a further temperature increase, the preference for the  $a$  sites decreases quite

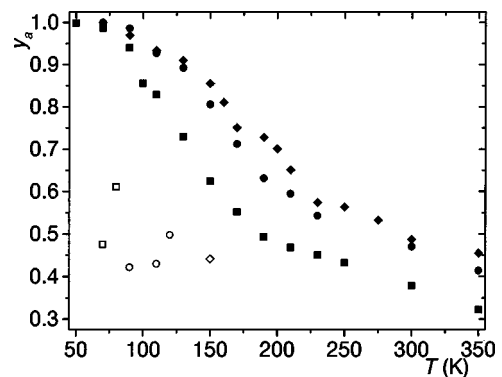


FIG. 2. The occupation ratio  $y_a$  as a function of temperature at  $x=0.05$  for three different pressures:  $p=4$  ( $\square$ ),  $7$  ( $\circ$ ), and  $10$  GPa ( $\diamond$ ). The open symbols denote a stable  $\varepsilon^*$  phase, closed denote a stable  $\delta^*$  phase. Large and small closed symbols indicate that the initial configuration was the  $\delta_{\text{rot}}^*$  and  $\varepsilon^*$  phase, respectively.

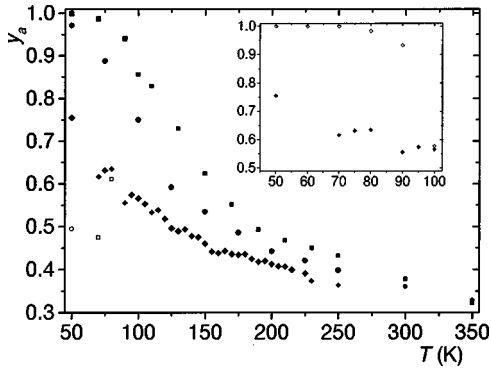


FIG. 3. The occupation ratio  $y_a$  as a function of temperature at  $p=4$  GPa for three different compositions:  $x=0.05$  ( $\square$ ),  $0.15$  ( $\circ$ ), and  $0.25$  ( $\diamond$ ). Open symbols denote a stable  $\varepsilon^*$  phase; closed symbols denote a stable  $\delta^*$  phase. Large and small closed symbols indicate that the initial configuration was the  $\delta_{\text{rot}}^*$  and  $\varepsilon^*$  phase, respectively. The inset shows the difference between the  $\delta_{\text{loc}}^*$  data (open symbols) and the data for the  $\delta_{\text{oo}}^*$  structure (closed).

rapidly. Around a certain temperature (about 180, 200, and 230 K for the respective pressures), the rate of decrease becomes smaller, and only a small decrease towards a complete random distribution is seen.

For later comparison with the experiments (see discussion), we performed additional simulations in the low- $T$  range where the  $\varepsilon^*$  phase remained stable (the open symbols in Fig. 2), but now taking a well-equilibrated configuration from a simulation at 7 GPa and 250 K for pure  $\text{N}_2$  ( $\delta_{\text{rot}}$ ), as the initial configuration. For pure  $\text{N}_2$  and the mixture, the  $\delta^*$  crystal structure never transforms spontaneously to the  $\varepsilon^*$  phase upon lowering  $T$ . In this way we can investigate the behavior of  $y_a$  in the  $\delta^*$  phase at low  $T$ . The results are also indicated with closed symbols. Combining these low-temperature results with the high temperature  $\delta^*$  phase, we come to the following conclusions.

In the  $\delta^*$  phase, the low- $T$  data indicate a region of  $y_a$  values close to the maximum value of 1. Moreover, there is only a small temperature dependence of  $y_a$  in this  $T$  region (probably  $y_a \rightarrow 1$  for  $T < 50$  K). A similar behavior is present for the other two pressures investigated. Therefore, concerning the distribution of Ar atoms in the  $\delta^*$  phase, we can discriminate between three temperature regions. At low temperatures, the preference for the  $a$  sites is nearly complete and almost independent of  $T$ . Around about 80, 130, and 140 K for  $p=4, 7,$  and  $10$  GPa, respectively, the preference for the  $a$  sites decreases rapidly with temperature. Subsequently, the rate of decrease becomes much smaller. Higher pressures result in a stronger preference for the  $a$  sites.

Figure 3 shows the equilibrium distributions of the Ar atoms as a function of  $T$  for three different compositions at  $p=4$  GPa. As was also visible from Fig. 1, within the orientationally disordered phases, the preference of the Ar atoms for the  $a$  sites decreases with increasing Ar content.

The three regions of Ar distribution are also present for  $x=0.15$  within the  $\delta^*$  phase. At low  $T$ , the  $\varepsilon^*$  phase is stable; the  $\varepsilon^*$ - $\delta^*$  transition occurs at about 60 K. However, for  $x=0.25$ , the  $\varepsilon^*$  phase is not present. It has transformed into the  $\delta^*$  phase, even at the lowest temperatures investigated. Therefore, the  $\varepsilon^*$ - $\delta^*$  transition shifts to lower  $T$  with

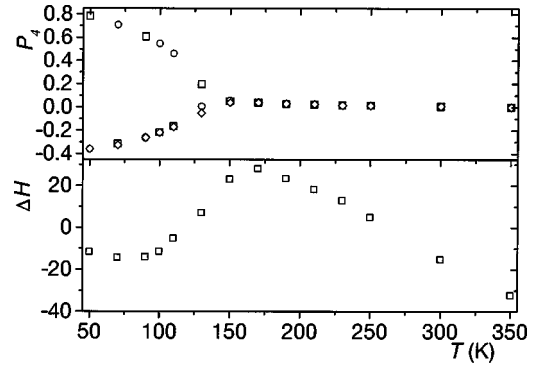


FIG. 4.  $O_\phi$  for the three different disks and  $\Delta H$  as a function of  $T$ , for  $x=0.05$  and  $p=4$  GPa.  $\Delta H$  denotes the difference between the calculated enthalpies  $H$  with the straight-line fit through the data. Only the data of the  $\delta^*$  phase are plotted. The errors are of the order of the symbol size.

increasing  $x$ . The long equilibration times pose a problem for the low temperature simulations, as was addressed in the previous section.

For the mixtures with 25% Ar, in particular with respect to the  $\delta_{\text{oo}}^*$  phase, metastability problems arise. These are similar to those in previous work: in a cooling run, the  $\delta_{\text{loc}}^*$  phase does not transform into another phase. At low temperatures, the  $\delta_{\text{oo}}^*$  phase appears spontaneously at 4 GPa, if we start with an initial distribution of Ar atoms over the  $a$  sites only. When starting with the Ar atoms initially distributed over the  $c$  sites only, the  $\delta_{\text{loc}}^*$  phase occurs, although in both cases the  $\varepsilon^*$  phase was taken as the initial structure. For these different phases, the equilibrium values of  $y_a$  are not equal, as is demonstrated in the inset of Fig. 3. As is clear from the figure the preference for the  $a$  sites of the Ar atoms is much stronger in the  $\delta_{\text{oo}}^*$  phase: for  $T \leq 70$  K, the Ar atoms do not migrate from the  $a$  to the  $c$  sites at all. When the  $\delta_{\text{oo}}^*$  phase is heated, the  $\delta_{\text{loc}}^*$  phase arises spontaneously, as in the heating runs without trial swap moves. The  $\delta_{\text{oo}}^*$ - $\delta_{\text{loc}}^*$  transition occurs at  $T=100$  K; at the transition,  $y_a$  has decreased drastically to the value of 0.58. In this work, at 4 GPa the  $\delta_{\text{oo}}^*$  phase appears only for  $x=0.25$ .

## B. Orientational delocalization

As in previous simulations, the orientational cascade process has been observed. The behavior is very similar to pure  $\text{N}_2$  (Ref. 3) and previous mixture results.<sup>8,17</sup> We refer to these results for a detailed explanation of the phenomena involved. The orientational delocalization is investigated with the order parameter  $O_\phi = \cos(4\phi)$ ,  $\phi$  being the disk angle in the plane of the disk (defined in Ref. 8). In Fig. 4, the order parameter and the enthalpy are shown as a function of  $T$  at  $x=0.05$  and  $p=4$  GPa. Below 150 K, the  $\delta_{\text{loc}}^*$  phase exists. At 150 K, the discrimination between the three disk types has disappeared, with this temperature we will identify the  $\delta_{\text{loc}}^*$ - $\delta_{\text{rot}}^*$  transition. Using the order parameter, for 7 and 10 GPa the transition temperatures are estimated at 190 and 250 K, respectively.

At 4 GPa, the  $\delta_{\text{loc}}^*$ - $\delta_{\text{rot}}^*$  transition occurs at about 150, 140, and 130 K for  $x=0.05, 0.15,$  and  $0.25$ , respectively. For pure simulated  $\text{N}_2$ , this transition occurs at about 150 K. This

TABLE I. The temperatures of the various transitions in the mixture.  $T_s$ : start of the increased rate of Ar redistribution  $T_e$ : end of this redistribution (both obtained from Fig. 2). Superscripts  $O_\phi$  and  $\Delta H$  denote that the transition temperature is obtained from curves of  $O_\phi$  and  $\Delta H$  versus  $T$ , respectively. The pressure is in GPa, and all temperatures are in K.

$p$	$T_s$	$T_e$	$T_{\delta_{loc}^*-\delta_{rot}^*}^{O_\phi}$	$T_{\text{onset}}^{\Delta H}$	$T_{\delta_{loc}^*-\delta_{rot}^*}^{\Delta H}$
4	80	180	150	90	170
7	130	200	190	130	210
10	140	230	250	175	250

suggests that the transition shifts slightly to lower temperatures with increasing  $x$ . This is in contrast to the simulations without performing trial swap moves, where the  $\delta_{loc}^*-\delta_{rot}^*$  transition was independent of composition. Nevertheless, the shift is small, and hardly detectable for the 5% mixture. The latter is also the case at higher pressures.

The rms displacement of the molecules with respect to the ideal crystallographic lattice sites has also been calculated. Because of the translation-rotation coupling, the orientationally localized disks have a different translational behavior than the other two disk types. The way this comes about in pure  $N_2$  and the mixtures has been discussed previously.<sup>17</sup> Again, at the  $\delta_{loc}^*-\delta_{rot}^*$  transition, the discrimination appears. The transition temperatures are the same as those obtained with  $O_\phi$ ; therefore the rms results are not shown here.

We have calculated the enthalpies for the various temperatures and pressures. At constant  $p$ , the enthalpy shows a nearly linear increase with  $T$ . The difference between the data points and a straight line fit through these points has been plotted in Fig. 4. As in pure  $N_2$  and previous mixture results, in the temperature region of orientational delocalization, the enthalpy shows a larger increase than the ordinary temperature effect above and below this region. Although the increased rate of Ar redistribution may have a contribution to this effect, the curve of  $\Delta H$  versus  $T$  can be used to make an estimate of the  $\delta_{loc}^*-\delta_{rot}^*$  transition temperature. Moreover, with these data one can observe the temperature at which the onset of the orientational delocalization occurs. The results are shown in Table I, together with the other relevant temperatures.

Although in this table the temperatures given are merely estimates, it suggests that there is an appreciable overlap between the regions of increased rate of Ar redistribution and the temperature region of orientational delocalization. Because of this overlap, it is not excluded that in the simulations the two processes are correlated, as will be discussed later.

### C. Unlike force field and other noble-gas atoms

In order to get more insight, we have performed additional simulations, in which a different redistribution behavior is obtained by modifying the three unlike exp-6 potential parameters in both directions. The Ar atoms showed a stronger preference for the  $a$  sites when there is a decrease in any of the three unlike exp-6 parameters, and vice versa. The results are most sensitive to a change in  $r_{ArN}^*$ , and least sen-

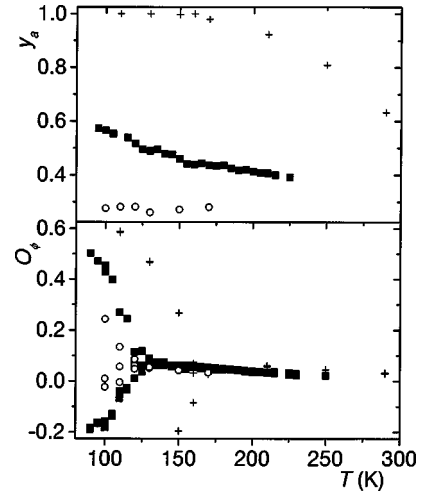


FIG. 5.  $y_a$  and  $O_\phi$  as a function of  $T$  for 25% argon at 4 GPa with a modified unlike site-site exp-6 parameter  $r_{ArN}^*$ . Given are the results with our original  $r_{ArN}^*$  (■),  $1.05r_{ArN}^*$  (○), and  $0.95r_{ArN}^*$  (+). Note that the first two data points for  $1.05r_{ArN}^*$  correspond with the  $\delta_{oo}^*$  phase.

sitive to a change in  $\epsilon_{ArN}^*$ , which suggests that, as in many other studies,  $r_{ArN}^*$  is the most relevant unlike parameter. The equilibration times also depend on  $r_{ArN}^*$ , and to a lesser degree on the two other parameters. This is not surprising, since a larger difference in molecular diameter will decrease the acceptance ratio, as is well known from similar techniques.<sup>10,18,19</sup>

For the 25% mixture we have performed simulations with  $r_{ArN}^* \rightarrow 0.95r_{ArN}^*$  and  $r_{ArN}^* \rightarrow 1.05r_{ArN}^*$  at several temperatures. We have chosen such a large change in the potential parameters to obtain an unambiguous result. The results are shown in Fig. 5. In the case of the smaller  $r_{ArN}^*$ ,  $y_a$  remains high, even for temperatures above the  $\delta_{loc}^*-\delta_{rot}^*$  transition. The rapid Ar redistribution occurs between about 200 and 400 K at a much smaller rate. The increase in  $r_{ArN}^*$  leads to a random distribution of Ar atoms over the lattice sites, even for low temperatures. For this mixture, there is an influence on the  $\delta_{loc}^*-\delta_{rot}^*$  transition. For  $r_{ArN}^* \rightarrow 0.95r_{ArN}^*$ , the  $\delta_{loc}^*-\delta_{rot}^*$  transition has shifted from about 130 to 170 K. In this case the increased rate of redistribution and the orientational delocalization do not overlap anymore. For the increased  $r_{ArN}^*$ , the  $\delta_{loc}^*$  phase does not exist above 110 K. Thus, the redistribution does affect the orientational delocalization and the  $\delta_{loc}^*-\delta_{rot}^*$  transition, but the reverse is not the case. For the 5% mixture, the distribution behavior is similar, but it hardly results in a shift of the  $\delta_{loc}^*-\delta_{rot}^*$  transition.

If indeed  $r_{ArN}^*$  is the most relevant unlike interaction parameter, one can make rough predictions about the behavior of the preferential distributions of other noble-gas atoms dissolving in  $\delta^*-N_2$ : for smaller atoms, the preference for the  $a$  sites will increase. Experimental results indicate that Ne, Ar, and Xe substitutionally dissolve into  $\delta^*-N_2$ .<sup>20,6,5</sup> Simulations with four different atomic species were performed. The results, shown in Table II, indeed indicate that for our potential model smaller molecules have a stronger preference for the  $a$  sites. During the simulations, the  $\epsilon^*$  structure transformed to the  $\delta_{rot}^*$  structure for all mixtures. This table sug-

TABLE II. Equilibrium results of the noble-gas distribution over the lattice sites at the state point ( $T=410$  K,  $p=7$  GPa,  $x=0.05$ ), for models of various noble-gas atoms. The exp-6 potential parameters  $\epsilon$  (well depth),  $\alpha$  (steepness at small  $\tau$ ), and  $r_{\text{ArN}}^*$  (atomic radius) are given for comparison, also for the  $\text{N}_2$ . The Ar and  $\text{N}_2$  parameters are taken from (Ref. 21), and the other values are taken from (Ref. 22).

Element	$\epsilon$ (K)	$\alpha$	$r^*$ (Å)	Diameter ratio	$y_a$
Ne	38.0	14.5	3.15	0.77	0.61
Ar	122.0	13.0	3.85	0.94	0.38
Kr	158.8	12.3	4.06	0.99	0.26
Xe	231.2	13.0	4.45	1.09	0.10
$\text{N}_2$	101.9	13.0	4.09	1.00	...

gests that the Kr atoms hardly show a preference for either the  $a$  or  $c$  sites, while Xe atoms preferentially occupy the  $c$  sites.

#### IV. DISCUSSION

For comparison, we have converted the experimentally obtained integrated intensity ratio<sup>6</sup>  $W$  into  $y_a$ , using  $y_a = (1 - 4W)/4x$ ; see Fig. 6. The experimental phase diagram<sup>6</sup> suggests that at least 25 mol% Ar dissolves into  $\delta^*-\text{N}_2$ . For relatively low temperatures,  $y_a$  is nearly independent of  $T$ , but at higher temperatures the Ar preference for the  $a$  sites decreases sharply. Moreover, the preference for the  $a$  sites increases with pressure. A comparison with Fig. 2 shows that the experiments and the simulation results within the  $\delta_{\text{loc}}^*$  phase agree qualitatively. In addition we have found that at even higher temperatures, possibly outside the experimental range, the rate of redistribution decreases again.

It is likely that the increased rate of redistribution corresponds with the experimentally obtained increase in the integrated intensity ratio, as we have found in the simulations. Both occur over a range of about 100 K. However, in experiments the redistribution starts just above the  $\delta_{\text{loc}}^*-\delta_{\text{rot}}^*$  transition, i.e., at a higher temperature. This might be due to the erroneous modeling of the Ar-N interactions, as is supported by the investigation of the influence of the potential parameters on the Ar distribution. Therefore, we have compared the ad hoc exp-6 potential used in this work with various recently developed  $\text{N}_2$ -Ar potentials.<sup>23-26</sup> In most of these papers, functional forms for the potential are given, with parameters fitted to *ab initio* potential energy surfaces and/or experimental data. The comparison shows that, depending on the model and the orientation of the  $\text{N}_2$  molecule, with our potential model in most cases the effective radius of the argon atoms is overestimated compared to the sophisticated models by 1% to 2%, leading to a smaller and less realistic preference for the  $a$  sites by the Ar atoms. However, although the repulsive wall is stated to be about correct for some models, no high-density data were used for these potentials. The exp-6 effective pair potential we have used is computationally convenient.

For low temperatures and high pressures, two different phases are obtained, depending, e.g., on the initial atomic distribution over the lattice sites. For small  $x$ , the  $\epsilon^*$  and  $\delta_{\text{loc}}^*$  phases both remain stable, while in the  $\delta^*$  phase the prefer-

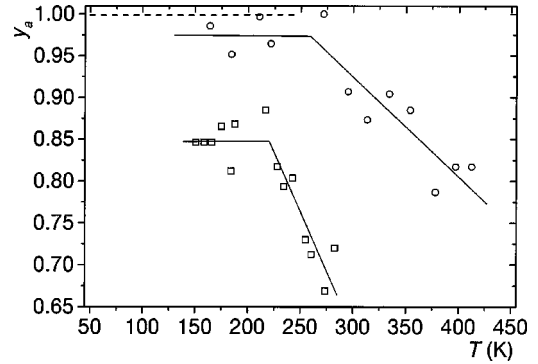


FIG. 6.  $y_a$  as a function of  $T$  as obtained from the experimental data (Ref. 6). The dots concern the 25 mol% mixture, at 5.5 GPa ( $\square$ ) and 11 GPa ( $\circ$ ). The dashed line indicates the results for the 15 mol% mixture at 6.7 GPa. The solid lines are guides to the eye.

ence of the Ar atoms for the  $a$  sites is much stronger than in the  $\epsilon^*$  phase. One of the two phases must be metastable. For large  $x$ , the  $\delta_{\text{loc}}^*$  and  $\delta_{\text{oo}}^*$  phases both remain stable. Here, the  $\delta_{\text{oo}}^*$  phase corresponds to the largest  $y_a$  value. Again, one of the two must be metastable. The differences between the structures are mainly orientational in nature. In both cases, a change in orientational behavior is accompanied by a change in distribution behavior. In the first case ( $\epsilon^*-\delta_{\text{loc}}^*$ ), an increase in orientational disorder corresponds to a decrease in configurational disorder, while in the second case ( $\delta_{\text{oo}}^*-\delta_{\text{loc}}^*$ ), an increase in orientational order corresponds to an increase in configurational order. Therefore, there is no simple relation between orientational order and the distribution of the Ar atoms.

For several compositions, experimental measurements have been performed down to 130 K for pressures up to 14 GPa (Ref. 6) and up to 25 GPa at room temperature (Ref. 5). For these conditions, the  $\epsilon^*-\delta^*$  transition has not been detected, which is in agreement with our results: In the simulations, the  $\epsilon^*-\delta^*$  transition shifts to lower  $T$  with increasing  $x$ . Also in previous simulations,<sup>8</sup> where the Ar atoms were distributed randomly over the  $a$  sites and no trial swap moves were performed, the  $\epsilon^*-\delta^*$  transition shifted to lower  $T$ . But in those simulations, at 7 GPa the transition occurs at around 60 K for  $x=0.05$ , while at that pressure and composition it occurs at about 125 K when trial swap moves are performed. One can conclude that a restriction of the Ar atoms to the  $a$  sites destabilizes the  $\epsilon^*$  structure: It is stable only if a significant amount of Ar atoms are distributed over the  $c$  sites.

Similarly, for  $x=0.25$ , the  $\delta_{\text{oo}}^*$  phase is stable only if a large number of Ar atoms is located at the  $a$  sites. This phase as well as the  $\delta_{\text{loc}}^*$  phase is stable at low temperatures. The preference for the  $a$  sites seems to be overestimated in the  $\delta_{\text{oo}}^*$  structure, while for the low-temperature  $\delta_{\text{loc}}^*$  phase,  $y_a$  has values that are in agreement with the experimental values (compare Figs. 3 and 6). On the other hand, the  $\delta_{\text{oo}}^*$  phase exhibits the low- $T$  dependence found in experiments (Ar distribution independent of  $T$ ).

Since the enthalpy is lowest when all Ar atoms are located at the  $a$  sites, it must be an entropy effect that, within the  $\delta^*$  phase,  $y_a$  decreases with increasing  $x$  at constant  $p$  and  $T$ . The dependence of  $y_a$  on  $x$  might indeed be a configurational

TABLE III. The enthalpy of the  $N_2$ -“Ar” mixture at  $T=410$  K,  $p=7$  GPa,  $x=0.05$  (the  $\delta_{\text{rot}}^*$  phase) for various values of the exp-6 parameter value  $r_{\text{ArN}}^*$ , as is indicated by the factor in the first column. In these simulations no trial swap moves were performed. The enthalpies are relative to the values at the  $a$  sites for  $r_{\text{ArN}}^* \rightarrow 0.95r_{\text{ArN}}^*$  ( $H=15\,322$  K).

	$a$	$r$	$c$
0.95	0	49	59
1	178	189	199
1.05	412	378	373
1.1	685	600	594
1.15	956	887	859

entropy effect, i.e., the disorder due to the mixing of the two types of molecules. The difference in configurational entropy between a distribution over the  $a$  sites only and a distribution over all the sites increases with  $x$ . We assume that a different atomic distribution does not influence other contributions to the configurational entropy or the thermal entropy of the system.

On the other hand, we attribute the increase in  $y_a$  as a function of  $p$  to the increase in the  $pV$  term of the enthalpy. Since the preference for the  $a$  sites by the Ar atoms is enthalpy-driven, one may expect that this driving force is larger for higher pressures.

The preference for the  $a$  sites shows a similar dependence for changes in any of the three unlike parameters. This may be explained by looking at the shape of the exp-6 potential. One should keep in mind that, for high pressures, the short-range, repulsive part of the potential is the most relevant part. The Ar- $N_2$  interaction is the most dominant interaction for the Ar atoms, being mainly located at the  $a$  sites, of which the nearest neighbors are  $N_2$ -occupied  $c$  sites. The simulations indicate that the Ar-N interaction is indeed repulsive: the largest molecular nearest-neighbor distance is about  $3.5$  Å (at 4 GPa, 100 K, 5% Ar). Decreasing  $\alpha_{\text{ArN}}^*$  (by 5%) leads to a slope that is less steep in the short-range repulsion: Defining the effective radius of the Ar atoms as the distance at which the Ar-N interaction is 300 K, this radius decreases by 1.0% if  $\alpha_{\text{ArN}}^*$  is decreased by 5%. A similar decrease in  $\epsilon_{\text{ArN}}^*$  leads to a decrease in the radius of 0.3%. Thus indeed,  $r_{\text{ArN}}^*$  and  $\epsilon_{\text{ArN}}^*$  have the largest and smallest influence, respectively, on the effective atomic radius, and a corresponding influence on the atomic distribution over the lattice sites.

From experiments, it can be deduced that at most 10 mol % neon dissolves into  $\delta^*$ - $N_2$ .<sup>6</sup> In this phase, the intensity ratio of the sphere and disk peak is  $0.24 \pm 0.03$ . The experimental accuracy was not high enough to determine the  $p$  and  $T$  dependence. If we assume that 10 mol % Ne dissolves into  $\delta^*$ - $N_2$ , then for an intensity ratio of 0.21 (the lower limit, note the error bar),  $y_a=0.6$ . However, if less Ne dissolves into solid  $N_2$ ,  $y_a$  is larger. We conclude that  $y_a \geq 0.6$ . Note that for an intensity ratio of 0.27 (the upper limit) and  $y_a=1$ ,  $x_{\text{Ne}}$  would be 0.05. Therefore, given the intensity ratio of the two peaks, at least 5 mol % Ne dissolves into  $\delta^*$ - $N_2$ . Since in these experiments the exact amount of Ne that dissolves into  $\delta^*$ - $N_2$  is not determined, it is not known whether, experimentally, the preference of the Ne at-

TABLE IV. The enthalpy at  $T=410$  K,  $p=7$  GPa,  $x=0.05$  (the  $\delta_{\text{rot}}^*$  phase) for mixtures of  $N_2$  with various noble gases, as modeled with the exp-6 parameters of Table II. No trial swap moves were performed. Values are relative to the values at the  $a$  sites for neon ( $H=15\,225$  K).

	$a$	$r$	$c$
Ne	0	52	65
Ar	272	293	283
Kr	385	381	386
Xe	742	700	682

oms for the  $a$  sites is smaller or stronger than that in the Ar case. However, the preference is very high.

Xe- $N_2$  has been investigated in the pressure range  $6 < p < 13$  GPa at  $T=408$  K, far above the pure  $N_2$   $\delta_{\text{loc}}^* - \delta_{\text{rot}}^*$  transition temperature. The integrated intensity ratio gives a value of  $0.28 \pm 0.03$ , while at least 16 mol % dissolves into  $\delta^*$ - $N_2$ . This corresponds to  $0.25 \leq y_a \leq 0.59$  (taking the error bars into account), which is smaller than that for Ne or Ar. We conclude that in the experiments the Xe atoms have a smaller preference for the  $a$  sites than the Ar and the Ne atoms. This is in qualitative agreement with the simulations. However, from experiments it is clear that the Xe atoms do show a preference for the  $a$  sites.<sup>20</sup> Therefore, in the simulations, the Ar as well as the Xe preference for the  $a$  sites should be much stronger in order to be in agreement with experiments. Also for Xe, this deviation might be due to the failure of the Lorentz-Berthelot mixing rule.

The enthalpy has been calculated for three values of  $r_{\text{ArN}}^*$  and for three distributions of the Ar atoms over the lattice. The results are shown in Table III. The positive enthalpy difference between the molecules at the  $c$  sites and the molecules at the  $a$  sites is larger for decreasing  $r_{\text{ArN}}^*$ . Thus, the increase in preference for the  $a$  sites with decreasing atomic size is most probably an enthalpy effect. For  $r_{\text{ArN}}^* \rightarrow 1.05r_{\text{ArN}}^*$  the difference has become negative: Here the smallest enthalpy is obtained when the atoms are distributed over the  $c$  sites. Table IV shows a similar trend: Smaller molecules have the smallest value of the enthalpy for the  $a$  sites, which indicates that the atomic size indeed is the most important property with regard to a preference for the lattice sites.

The behavior of the  $\delta_{\text{loc}}^* - \delta_{\text{rot}}^*$  transition for the modified values of  $r_{\text{ArN}}^*$ , as shown in Fig. 5, is consistent with the ideas about the location of the  $\delta_{\text{loc}}^* - \delta_{\text{rot}}^*$  transition as a function of  $x$ .<sup>8</sup> For the simulations with the Ar atoms restricted to the  $a$  sites, it was argued that the  $\delta_{\text{loc}}^* - \delta_{\text{rot}}^*$  transition temperature is independent of  $x$ , since it is the disk molecules (at the  $c$  sites) that participate in the orientational delocalization. As soon as a considerable amount of Ar is present at the  $c$  sites, one might expect that the distribution does affect the orientational delocalization. For  $r_{\text{ArN}}^* \rightarrow 1.05r_{\text{ArN}}^*$ , the Ar atoms are randomly distributed over all the lattice sites, and when  $x$  is relatively large, a reasonable fraction of the  $c$  sites is occupied by Ar atoms. This may enhance the orientational cascade process, which will shift the  $\delta_{\text{loc}}^* - \delta_{\text{rot}}^*$  transition to lower temperatures. Indeed, this transition occurs at about 115 K, while it occurs at about 150 K for pure  $N_2$ . In the simulations

with the original potential parameters, the increased rate of Ar redistribution and the orientational cascade process overlap. There, the redistribution may already lower the  $\delta_{\text{loc}}^* - \delta_{\text{rot}}^*$  transition temperature by the migration of atoms from the  $a$  to the  $c$  sites. This is probably the cause of the small shift in the  $\delta_{\text{loc}}^* - \delta_{\text{rot}}^*$  transition as a function of  $x$ . Therefore, we conclude that the distribution of Ar atoms has some influence on the orientational delocalization and on the  $\delta_{\text{loc}}^* - \delta_{\text{rot}}^*$  transition.

On the other hand, for  $r_{\text{ArN}}^* \rightarrow 0.95r_{\text{ArN}}^*$ ,  $y_a$  remains high up to temperatures way above the  $\delta_{\text{loc}}^* - \delta_{\text{rot}}^*$  transition. We therefore conclude that the orientational delocalization does not have much influence on the distribution of Ar atoms over the lattice sites.

In order to obtain results in the high-pressure, low-temperature regions, we have attempted to obtain an additional speed-up in the calculations. First, in combination with the orientational bias, we tried a similar bias in which pairs of unlike molecules were chosen. A pair with the smallest increase in energy had the largest probability to be selected. Second, we have tried to reduce the number of calculations that are performed in the selection of the orientation by introducing a second cutoff radius.<sup>27</sup> Neither of the techniques resulted in a significant speed-up of the calculations, although it may prove to be beneficial after a more elaborate fine-tuning of the parameters involved, or for larger system sizes.

## V. CONCLUSIONS

For not too large pressures and too low temperatures, the technique in which the identity of two molecules has been changed simultaneously in  $(N,p,T)$  simulations can be successfully applied. An orientational bias must be included in order to make the CPU time per accepted swap move practicable. With this method, the preference of (argon) atoms for either of the two lattice sites of high-pressure  $\text{N}_2$  can be investigated.

In the  $\varepsilon^*$  as well as the  $\delta^*$  phase, the Ar atoms preferentially occupy the  $a$  sites. The  $\varepsilon^* - \delta^*$  transition shifts to lower  $T$  with increasing  $x$ , but at a much smaller rate than in previous simulations in which the Ar atoms were restricted to the  $a$  sites. Therefore, a large preference for the  $a$  sites destabilizes the  $\varepsilon^*$  phase. At the  $\varepsilon^* - \delta^*$  transition, there is a significant increase in the preference for the  $a$  sites. Since in experiments the  $\varepsilon^*$  phase has not been detected, and since for the  $\delta_{\text{loc}}^*$  phase the preference for the  $a$  sites is in much better agreement with experiments, we suggest that the  $\varepsilon^*$  phase is metastable with respect to the  $\delta^*$  phase.

Within the  $\delta^*$  phase, at low temperatures the Ar atoms exhibit a nearly complete preference for the  $a$  sites, hardly dependent on  $T$ . Above a certain temperature, the Ar atoms redistribute rapidly. At even higher temperatures, a slow redistribution towards a random distribution occurs.

For  $x=0.05$ , this behavior is the same for all pressures

investigated, while a higher pressure results in a stronger preference for the  $a$  sites. For  $x=0.15$ , the behavior is similar, although the preference decreases with increasing  $x$ . This is an entropy effect, since the enthalpy is smallest when the Ar atoms are distributed over the  $a$  sites only. Both the pressure and temperature dependence are in qualitative agreement with experiments. Although the experimental accuracy is not very high, the largest quantitative discrepancy lies in the temperature at which the Ar atoms start to redistribute. The simulations give a value that is too low. This is most likely due to an erroneous modeling of the unlike exp-6 parameters: These are probably chosen too large.

There is no immediate influence of the orientational (dis)order on the configurational (dis)order related to the distribution of atoms. First, this is demonstrated by the difference in distribution at the transitions between the high-pressure phases. At the  $\varepsilon^* - \delta_{\text{loc}}^*$  transition, the orientational order decreases, while the configurational order increases. On the other hand, at the  $\delta_{\text{oo}}^* - \delta_{\text{loc}}^*$  transition, the orientational as well as the configurational disorder increases. Second, the orientational delocalization, resulting in the  $\delta_{\text{loc}}^* - \delta_{\text{rot}}^*$  transition, has no influence on the distribution of the atoms.

In contrast, there is an influence of the configurational (dis)order on the orientational (dis)order. The  $\delta_{\text{loc}}^* - \delta_{\text{rot}}^*$  transition shows a small shift to lower  $T$  with increasing  $x$ . This is most probably due to the occupation of Ar atoms at the  $c$  sites, which increases with increasing  $x$ . The  $\text{N}_2$  molecules at the  $c$  sites are responsible for the orientational delocalization. The Ar atoms at the  $c$  sites probably enhance this effect.

An investigation of the potential parameters shows that a decrease in any of the three unlike exp-6 parameters results in a stronger preference for the  $a$  sites, since such a decrease results in a decrease in the effective atomic radius. Relative changes in  $r_{\text{ArN}}^*$  and  $\varepsilon_{\text{ArN}}^*$  have the largest and smallest influence, respectively. As a consequence of this behavior, the increased rate of Ar redistribution occurs at a much higher temperature for smaller molecules.

Another consequence is that smaller noble-gas atoms have a stronger preference for the  $a$  sites. The increase in preference for the  $a$  sites as the diameter decreases can be accounted for by the larger enthalpy differences. Although the experimental accuracy is poor, the simulation results for the different molecules agree qualitatively with experimental data. The preference for the  $a$  sites is underestimated in all cases; again this may be due to an incorrect unlike interaction model.

## ACKNOWLEDGMENTS

This work was financially supported by the Stichting Fundamenteel Onderzoek der Materie (FOM). A part of the computer resources has been provided by the Stichting Academisch Rekencentrum Amsterdam (SARA). We would like to thank Berend Smit and Hans Bakker for useful discussions.

\*Electronic address: klaveren@phys.uva.nl

<sup>1</sup>V. G. Manzhelii and Y. A. Freiman, *Physics Of Cryocrystals* (AIP, New York, 1997).

<sup>2</sup>M. I. M. Scheerboom and J. A. Schouten, *Phys. Rev. Lett.* **71**, 2252 (1993).

<sup>3</sup>A. Mulder, J. P. J. Michels, and J. A. Schouten, *Phys. Rev. B* **57**, 7571 (1998).

<sup>4</sup>M. Hanfland, M. Lorenzen, C. Wassiliw-Reul, and F. Zontone, *Rev. High Pressure Sci. Technol.* **6**, 130 (1997).

<sup>5</sup>T. Westerhoff and R. Feile, *Phys. Rev. B* **54**, 913 (1996)

- <sup>6</sup>M. E. Kooi and J. A. Schouten, *Phys. Rev. B* **57**, 10 407 (1998).
- <sup>7</sup>E. P. van Klaveren, J. P. J. Michels, and J. A. Schouten, *J. Low Temp. Phys.* **111**, 413 (1998).
- <sup>8</sup>E. P. van Klaveren, J. P. J. Michels, and J. A. Schouten, *Mol. Phys.* **96**, 1613 (1999).
- <sup>9</sup>A. D. Kofke and E. D. Glandt, *Mol. Phys.* **64**, 1105 (1998).
- <sup>10</sup>D. Frenkel and B. Smit, *Understanding Molecular Simulation* (Academic, San Diego, 1996).
- <sup>11</sup>R. F. Cracknell, D. Nicholson, N. G. Parsonage, and H. Evans, *Mol. Phys.* **71**, 931 (1990).
- <sup>12</sup>M. Parinello and A. Rahman, *Phys. Rev. Lett.* **45**, 1196 (1980).
- <sup>13</sup>M. Parinello and A. Rahman, *J. Appl. Phys.* **52**, 7182 (1981).
- <sup>14</sup>M. P. Allen and D. J. Tildesley, *Computer Simulation of Liquids* (Clarendon, Oxford, 1986).
- <sup>15</sup>H. Flyvbjerg and H. G. Petersen, *J. Chem. Phys.* **91**, 461 (1989).
- <sup>16</sup>R. D. Eppers, V. Chandrasekharan, E. Uzan, and K. Kobashi, *Phys. Rev. B* **33**, 8615 (1986).
- <sup>17</sup>E. P. van Klaveren, J. P. J. Michels, and J. A. Schouten, *Int. J. Mod. Phys. C* **10**, 445 (1999).
- <sup>18</sup>W. G. T. Kranendonk and D. Frenkel, *Mol. Phys.* **72**, 679 (1991).
- <sup>19</sup>W. G. T. Kranendonk and D. Frenkel, *Mol. Phys.* **72**, 699 (1991).
- <sup>20</sup>M. E. Kooi and J. A. Schouten, *Phys. Rev. B* **60**, 12 635 (1999).
- <sup>21</sup>F. H. Ree, in *Simple Molecular Systems at Very High Density*, edited by A. Polian, P. Loubeyre, and N. Boccara (Plenum, New York, 1988), p. 153.
- <sup>22</sup>J. O. Hirschfelder, C. F. Curtiss, and R. B. Bird, *Molecular Theory of Liquids and Gases* (Wiley, New York, 1967).
- <sup>23</sup>B. Fernández, H. Koch, and J. Makarewicz, *J. Chem. Phys.* **110**, 8525 (1999).
- <sup>24</sup>F. Y. Naumkin, *Mol. Phys.* **90**, 875 (1997).
- <sup>25</sup>A. K. Dahm, F. R. W. McCourt, and W. J. Meath, *J. Chem. Phys.* **103**, 8477 (1995).
- <sup>26</sup>L. Beneventi, P. Casavecchia, G. G. Volpi, C. C. K. Wong, and F. R. W. McCourt, *J. Chem. Phys.* **98**, 7926 (1993).
- <sup>27</sup>T. J. H. Vlugt, M. G. Martin, B. Smit, J. I. Siepmann, and R. Krishna, *Mol. Phys.* **94**, 727 (1998).